Resilient Cities and Structures 1 (2022) 87–96

Contents lists available at ScienceDirect

Resilient Cities and Structures

journal homepage: www.elsevier.com/locate/rcns

An overarching framework to assess the life-time resilience of deteriorating transportation networks in seismic-prone regions

Alice Alipour*, Behrouz Shafei

Department of Civil, Construction, and Environmental Engineering, Iowa State University, Ames, IA 50011, USA

ARTICLE INFO

Keywords:
Resilience assessment
Transportation networks
Aging bridges
Deterioration
Functionality measures

ABSTRACT

This study develops a comprehensive framework to assess the resilience of transportation networks consisting of deteriorating bridges subjected to earthquake events. For this purpose, the structural capacity of highway bridges is estimated during their service life using a set of detailed finite-element models that simulate the progress of deterioration. The developed models take into consideration the main environmental stressors and determine the extent of capacity loss as a function of time. Based on the degraded state of structural components, seismic fragility analyses are performed to obtain a probabilistic evaluation of the extent of damageability of the existing bridges under seismic events. Since each transportation link normally consists of a number of bridges, the state of damage in the individual bridges is mapped to the corresponding links and a scenario-based approach is employed to estimate the resilience of the entire transportation network. To demonstrate how the consequences of structural degradation can be integrated into the developed framework, the large-scale transportation network of Los Angeles and Orange counties is investigated under a series of aging and earthquake scenarios. The outcome of this study indicates how the estimates associated with the functionality measures of a transportation network can be improved if the age factor is properly integrated into the framework used for resilience assessment.

1. Introduction

The performance assessment of transportation networks under extreme events has been an issue of concern for engineers and decision-making authorities who work on civil infrastructure systems. A critical aspect that makes transportation networks different from the other constructed facilities is the spatial distribution and connectivity of network components. This aspect creates sensitivity, especially to the consequences of natural and manmade hazards, as disruptions in only a few components may result in detrimental effects on the functionality of the entire network. The importance of maintaining a resilient transportation network can be recognized during both normal operation and emergency situations. Among various extreme events that a transportation network can experience, earthquakes are found to have the most destructive effects, as they often impact a significant portion of the network at the same time. While a transportation network consists of several components, bridges are identified as the most expensive, yet most vulnerable components. The extent of vulnerability of bridges is reflected in the average age of existing bridges (e.g., 45 years for the bridges in the United States) and their continuous exposure to severe climatic conditions [1]. The environmental stressors, including temperature and humidity variations, attack of corrosive agents due to airborne or deicing salts, and acidic rains in polluted urban regions, may significantly degrade the integrity of structural components and magnify the extent of damage caused by sudden extreme loads.

There are several studies in the literature that have investigated the reduced functionality of transportation networks under extreme events (e.g., [2–7]). However, most of the available studies have assumed that the bridges that serve a transportation network are in a pristine condition with no degradation. This assumption is not always accurate, as it is known that aging mechanisms may adversely affect the structural capacity and performance of bridges (e.g., [8–15]). The capacity loss of reinforced concrete (RC) bridge components due to corrosion and the subsequent effects on the seismic response of highway bridges have been examined by Alipour et al. [16] through a computational framework. This framework provides a probabilistic approach to predict possible changes in seismic fragility measures by taking into account the age factor, in addition to site-specific exposure conditions. This and similar studies conducted at the component level have led researchers to investigate the effects of aging mechanisms on the post-earthquake functionality of the entire transportation network. For example, Lee et al. [17] used a matrix-based system reliability method to estimate changes in the flow capacity of a network of deteriorated bridges; Rokneddin

* Corresponding author.
E-mail addresses: alipour@iastate.edu (A. Alipour), shafei@iastate.edu (B. Shafei).

https://doi.org/10.1016/j.rcns.2022.07.002
Received 12 May 2022; Received in revised form 30 June 2022; Accepted 12 July 2022

et al. [18] assessed the reliability of a degraded transportation network under moderate seismic risk; Alipour et al. [19] studied the direct and indirect costs associated with a highway network consisting of aged bridges through different bridge-age scenarios; Singh et al. [20] provided a procedure to quantify resilience; Castillo et al. [21] developed a methodology to achieve resilience through improving individual structures; and Blagojevic and Stojadinovic [22] proposed a demand-supply framework to evaluate the effect of resource and service constraints on community disaster resilience.

Considering the wealth of knowledge currently available, the main objective of this study is to provide an overarching framework for the assessment of large-scale transportation networks subjected to regional hazards and deterioration mechanisms. For this purpose, the complex highway network of Los Angeles and Orange counties is modeled with actual origin-destination (OD) data. By utilizing trip assignment and traffic flow analyses, the functionality of this network is examined after a series of scenario earthquakes. These scenario earthquakes are selected to represent the seismic hazard risk of the region and provide the information required to determine the spatial distribution of seismic intensity measures. Based on the obtained site-specific seismic demand, the state of damage in various network components is calculated. To capture the contribution of aging mechanisms, the finite-element (FE) framework developed by Shafei et al. [23] is utilized. This helps predict the extent of deterioration of structural components at multiple time steps during the service life of the existing bridges. The functionality of the aging network is, then, evaluated under each scenario earthquake and comparisons are made with the results obtained from the network in the intact condition. The outcome of this study paves the way to identify appropriate risk mitigation strategies for existing transportation networks.

2. Research methodology

To establish a framework that can evaluate the life-time resilience of a transportation network, it is essential to identify appropriate performance measures capable of comparing the intact and deteriorated state of the network. Among various measures, the total travel time is used as the performance measure of choice in the current study. This measure is defined as the time required for all the vehicles that have initiated a trip in the network to reach their destinations in a specific time frame. Since the introduced measure takes into account the changes in the demand and pattern of traffic after an earthquake event, it can be employed as a reliable measure for various aging and earthquake scenarios. By calculating the total travel time in the network of intact bridges impacted by the s-th scenario earthquake, $TT_{0,s}$, the effects of aging mechanisms on the functionality of the network can be quantified by estimating the $TT_{t,s}$, which reflects the increase in the total travel time due to the damage incurred to the network components. To estimate the probability of exceeding the maximum acceptable travel time, the entire network is modeled at different levels of aging, and the age-dependent total travel times are calculated. This probability, $P(t, s)$, can be expressed as:

$$P(t,s) = P\left[TT_{c,s} \leq TT_{t,s}\right] \tag{1}$$

where t is the age of the network; s is the scenario earthquake number; and $TT_{c,s}$ is the critical threshold for the total travel time, beyond which the performance of the network is not acceptable. The critical total travel time is determined from a number of factors considered by decision-making authorities and can be adjusted based on the importance of the network. Alternatively, a maximum percentage of increase in the total travel time can be introduced, indicating that the functionality of an impacted network is not acceptable anymore if the total travel time reaches κ% higher than the intact condition. It should be noted that the total travel time has been recognized as a reliable measure to represent the overall performance of a transportation network. In some instances, however, other performance measures, including connectivity and link-specific travel time, can be desirable. Such performance measures are mostly suitable for local studies, in which the goal is to ensure the reachability and short commute time for certain links that are deemed critical to get to hospitals, fire stations, and shelters.

Under a major earthquake event, two main reasons can contribute to the underperformance of a transportation network: loss of capacity and increase in demand. A network's traffic capacity is determined based on the capacity of its individual components, especially bridges. Because of long-term deterioration, however, the damageability of several bridges can increase during seismic events. Considering the fact that each link of a transportation network normally consists of at least one bridge, any damage to the existing bridges can potentially lower the capacity of the network as a whole. On the other hand, demand on a transportation network increases over time, as the population grows and the number of vehicles in service increases. While the framework developed in this study is capable of examining the effects of both capacity and demand parameters, the presented results only focus on capacity evaluation, assuming no changes in the demand during the network's service life. This assumption helps illustrate the actual effects of aging on the functionality of deteriorating networks.

3. Life-time fragility analysis

A transportation network consists of several bridges, the performance of which plays a critical role in the functionality of the entire network, especially during extreme events. To assess the vulnerability of the existing bridges subjected to earthquake loads, the seismic fragility of each bridge should be estimated to identify the extent of damageability as a function of ground motion intensity. For this purpose, a set of four fragility curves that represent four different damage states are developed. The damage states are classified as (at least) slight, (at least) moderate, (at least) extensive, and complete collapse, following the definition provided by HAZUS-MH [24]. Based on the introduced damage states, the analytical fragility curves of the individual bridges are generated at different ages, prior to and after the initiation of deterioration. To perform fragility analyses, the curvature ductility of the bridge column is considered as the primary measure of damage. The curvature ductility is defined as the ratio of maximum column curvature recorded from a nonlinear time-history analysis to the column yield curvature obtained from the moment-curvature analysis. Following the procedure given by Priestley et al. [25], the curvature ductility of each bridge is calculated under a suite of ground motions and the results are compared to the limit states of damage. In this study, the damage limit states are assumed to equal the ductility of 1.0, 2.0, 4.0, and 7.0 for the slight, moderate, extensive, and complete damage states, respectively. The estimation of these limit states is beyond the scope of this study, but the suggested values are in accordance with the limit states available in the literature (e.g., [26,27]).

To create reliable finite-element (FE) models for the bridges under consideration, a number of parameters should be considered. These parameters determine (i) the material properties of structural elements (e.g., yield and ultimate strength of steel and compressive strength of concrete) and (ii) the geometric details of the bridge components (e.g., span length, deck section, column height, and rebar size). Given that the listed parameters may significantly vary from one bridge structure to another, depending on site-specific conditions and design and construction criteria, it is important to have a proper distribution of bridge types/details in the transportation network under consideration. Thus, a comprehensive study has been conducted on the bridges in California [28], categorizing them based on their age, dimensions, structural characteristics, and material properties. Since more than 85% of the bridges in California are made of concrete, this study focuses on RC bridges with different structural properties. Upon the identification of the most common types of RC bridges, a group of 18 representative bridge models with two and three spans have been modeled. The referenced bridge models have three variations in their span lengths (i.e., short-, medium-, and long-span). The modeled bridge decks consist of concrete box girders with a total concrete cross section of approximately

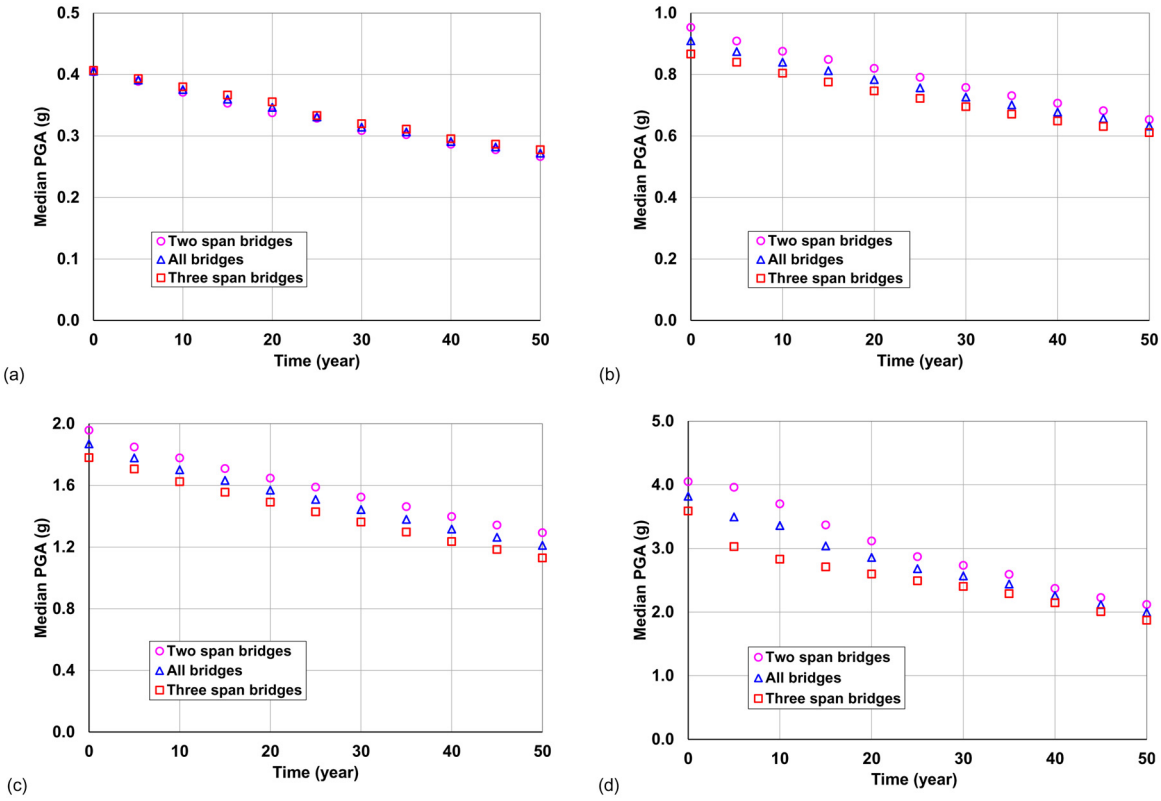

Fig. 1. Time-dependent median values of fragility curves obtained for the two- and three-span bridges under consideration: (a) minor, (b) moderate, (c) major, and (d) complete collapse damage state.

12 m^2. The bridges under study have interior bents with two circular columns that have identical diameters and heights. The column diameter varies from 1.5 to 1.9 m, depending on the bridge span length. Each of the short-, medium-, and long-span categories includes bridges with the column height of 7.5 m, 10.0 m, and 12.5 m. This provides a range of span length-to-column height ratios from 1.2 to 6.0 [29].

Durability of RC bridges is significantly impacted by the penetration of corrosive agents in concrete and the onset of corrosion in steel rebars. By increasing the time during which a bridge is exposed to aggressive conditions, the deterioration process of reinforcing bars can become relatively fast. This results in the cracking and spalling of the concrete cover, in addition to reduction in the mass and effective cross section of the reinforcing bars [30–33]. To evaluate the effects of deterioration on the lifetime performance of bridges, the extent of structural degradation is calculated over the life-cycle of each bridge case. The fragility curves are, then, generated for all the representative bridges at regular time intervals. Considering the extent of structural degradation, the fragility curves are estimated for all the deteriorating bridges through a procedure similar to that explained for the intact bridges [34]. To avoid the intersection of fragility curves, a similar standard deviation is assumed, following the recommendation made by Shinozuka et al. [35]. This helps capture the changes in the median values of fragility curves for all the bridge cases, as shown in Fig. 1. This figure indicates that the overall average of median values obtained for the four damage states decreases by 38% and 34% over 50 years for the two- and three-span bridges, respectively. With such a drop in the median of fragility curves, the probability of exceeding any damage state is expected to increase over time, primarily due to deterioration mechanisms. This consequently increases the seismic damageability of the existing bridges, making them potentially vulnerable to the seismic hazard risks that were originally deemed tolerable.

4. Scenario earthquakes and damage states

Los Angeles and Orange counties are located in a high-seismic region with many active faults and a large number of recorded ground motions. To evaluate the seismic risk that the transportation network experiences in this region, Chang et al. [36] identified a subset of scenario earthquakes that represent the seismic hazard of the entire region consistent with the USGS database. This set includes a total of 47 scenario earthquakes, including 13 maximum credible and 34 user-defined events [37]. It is important to note that a highway transportation network is a spatially distributed network, in which each of the network components can experience a different level of seismic excitation, depending on the earthquake's epicenter and site characteristics. Thus, an attenuation relationship is employed for each of the scenario earthquakes to estimate the peak ground acceleration (PGA) throughout the entire region served by the transportation network. An attenuation relationship is defined as a predictive correlation, which can be developed statistically from the historical ground motion records. This allows the estimation of ground motion intensity measures at a given distance from the epicenter of an earthquake with a known magnitude. Among all the attenuation relationships developed for the Western United States, the one proposed by Campbell and Bozorgnia [38] is used in the current study.

Since the seismic damageability of bridges is expressed in the form of fragility curves as a function of PGA, the attenuation relationship is utilized to estimate the PGA at each bridge site under the scenario earthquakes. Upon the determination of the site-specific PGA, the bridge damage state is identified and the probability of failure of the bridge under that damage state is calculated using the fragility parameters. This procedure is repeated for all the bridges in the network considering all the scenario earthquakes. The bridge damage state is, then, mapped to the

Table 1
Changes in the free flow speed and traffic capacity of the network links as a function of the link damage state.

Link Damage State	LDI Lower Bound	LDI Upper Bound	Free Flow Speed (%)	Traffic Capacity (%)
Minor	0.0	0.5	100	100
Moderate	0.5	1.0	75	100
Major	1.0	1.5	50	75
Collapse	1.5	∞	50	50

bridge damage index (BDI) defined according to the Caltrans report on the damage state of bridges after the Northridge earthquake. In the current study, the BDI is assumed to equal to 0.10, 0.30, 0.75, and 1.00 for the slight, moderate, extensive, and complete collapse states of damage, respectively [39]. The reason for converting the bridge damage state to the BDI is to compute the link damage state. Each link consists of a number of bridges and damage to any of them directly affects the performance of the entire link. Following the calculation of the BDI for all the network bridges, the link damage index (LDI) is estimated for each link as the square root of the sum of the squares (SRSS) of the BDIs obtained for the bridges located on that link. The LDI is found to increase at a decreasing rate when the number of damaged bridges on a given link increases. Based on the calculated LDIs, four states of damage are identified for each link. The link damage states are introduced similar to the bridge damage states using lower and upper bounds (Table 1). Based on the extent of damage to a link, modification factors are determined for the free flow speed and residual traffic capacity of the network links. The values assigned to these two parameters can be found in Table 1 [37].

5. Traffic assignment models

To study the functionality of a transportation network subjected to an earthquake event, it is essential to model the network's expected demand and capacity after the earthquake. For this purpose, two models have been commonly used: (i) fixed- and (ii) variable-demand. The fixed-demand model assumes that the demand between any origin and destination remains the same with no change after an earthquake. This model, however, is proven to be inadequate, as it may assign an unrealistically large demand to the network. As a case in point, the data collected by the Caltrans after the Northridge earthquake indicated that the traffic doubled on the routes near the collapsed bridges, which resulted in a 15 min increase of travel time per trip in comparison to the original pre-earthquake travel time. It was shown by Werner et al. [40] that the calculations made by the fixed-demand model overestimated the travel times by a factor of up to 10 for the same network. Fig. 2(a) conceptually depicts the fixed-demand model, where the demand curve is horizontal with no changes after an earthquake event. On the other hand, the capacity is expected to decrease after an earthquake event, as several links may not be functional anymore.

The variable-demand model assumes that the trip rates are influenced by the service level of a network. This means that after an earthquake, many drivers may not be willing to endure long travel times and instead forgo the trip or change their route or mode of traffic [40,41]. The category of variable-demand models can itself be divided into the linear and nonlinear models. In the linear models, the travel time linearly depends on the network's capacity. Fig. 2(b) illustrates that the transportation network has a capacity of C_1, which requires a travel time of t_1. However, when the capacity of the network decreases to C_2, due to an earthquake, the travel time increases to t_2. By comparing the difference between the travel times calculated before and after an earthquake using the fixed- and variable-demand models, it is noted that the variable-demand model typically results in a smaller yet more realistic increase within the travel time in a damaged network. This trend has been verified by Werner et al. [40]

There is also nonlinear variable-demand model, in which a nonlinear change is considered for both demand and capacity parameters. This

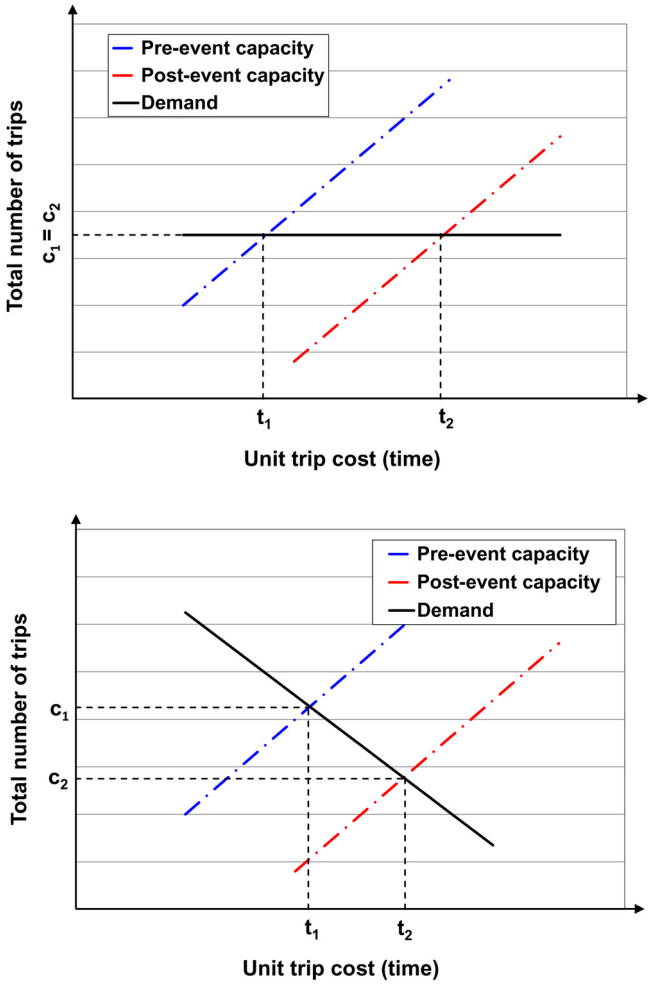

Fig. 2. Fixed-demand (top) and linear variable-demand (bottom) models as alternatives for traffic assignment.

model has been developed based on the fact that after an earthquake, a wide range of disruptions occur in business, commercial, industrial, and even cultural activities. Such disruptions are mainly because the structures that house everyday activities are damaged, and as a result, post-event activities are reduced. This situation drastically changes the OD data, as degradation in the overall network performance causes a significant reduction in the number of trips for the same trip cost. The trip reduction model is obtained based on a number of factors, including network configurations, damaged buildings in the network's service area, and reduction of associated activities. The contribution of all these factors can be expressed in the form of reduction rates for various trip purposes in each trip analysis zone. In this study, six general trip purposes are considered. The reduction rates assigned to the origin and destination of each of them (ξ_i^p and ξ_j^p) are given in Table 2 for different levels of earthquake magnitude.

Table 2
Trip reduction rates for the six different trip purposes [3].

Trip Purpose		Level of Ground Motion (Moment Magnitude) 6	7	8	9	10
Home-Work	Origin	0.032	0.26	0.743	5.537	14.441
	Destination	0.045	0.334	0.794	7.911	24.938
Home-Shop	Origin	0.032	0.26	0.743	5.537	14.441
	Destination	0.036	0.294	0.651	6.243	20.185
Home-Other	Origin	0.032	0.26	0.743	5.537	14.441
	Destination	0.043	0.329	0.769	7.422	23.548
Work-Other	Origin	0.045	0.334	0.794	7.911	24.938
	Destination	0.043	0.329	0.769	7.422	23.548
Other-Other	Origin	0.043	0.326	0.765	7.339	23.246
	Destination	0.043	0.326	0.765	7.339	23.246
Truck Trip	Origin	0.035	0.369	0.889	8.783	25.191
	Destination	0.035	0.369	0.889	8.783	25.191

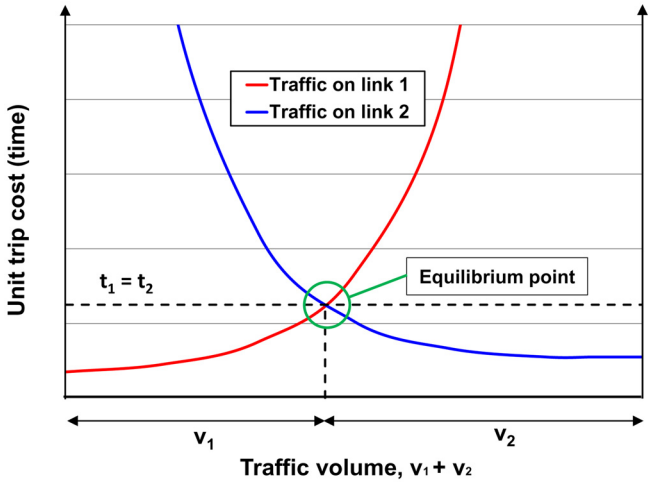

Fig. 3. Point of equilibrium in a simple network model with two nodes.

To simulate the transportation network of the region under study, a comprehensive traffic assignment model is utilized. This model estimates the expected travel volume and time of each link, following the Wardrop rules [42]. Based on the Wardrop rules for the equilibrium of a network, the travel time along the unused paths of a network is longer than that along the used paths. In addition, individual drivers are unable to improve their travel times further even by changing their routes. Considering the listed rules, the network assignment model adjusts the traffic volume and congested travel time of each path to reach the equilibrium condition. The equilibrium condition is achieved when the travel time on all the paths between any pair of OD becomes identical. This travel time can be accepted only if it equals to or becomes less than the travel time on any unused paths connecting the same OD pair.

To understand the concept of equilibrium, a very simple transportation network can be considered with only two nodes, where N drivers drive from the origin 1 to the destination 2 in two different paths of 1 and 2. The travel time, t_i, for each of these routes can be estimated based on the traffic volume of that route, v_i. At the equilibrium condition, the travel time along both paths is identical and the total number of drivers, N, is divided into two traffic volumes, v_1 and v_2, according to the equilibrium travel time, t_e. As reflected in Fig. 3, the area beneath these two functions is minimized for a given travel demand when the trips are divided so that the travel times on the path 1 and 2 are identical [40]. For the current study, the pre- and post-earthquake demand and capacity are depicted in Fig. 4. This figure shows that the degradation in the performance of the transportation network results in a reduced number of trips for the same unit trip cost or higher unit trip cost for the same number of trips. On the other hand, damage to the network components after an earthquake event causes a capacity loss

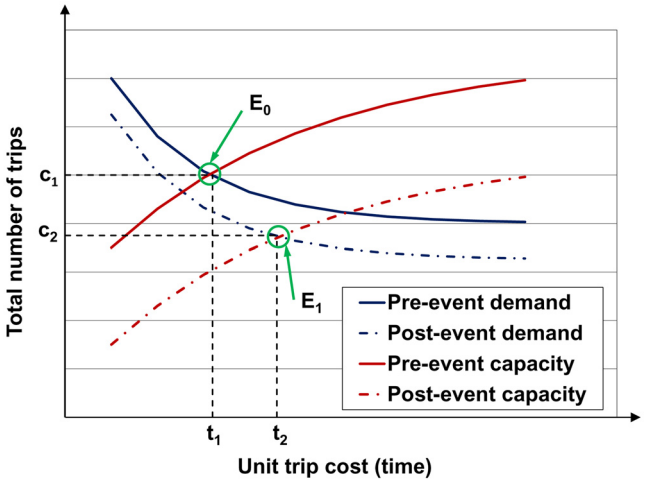

Fig. 4. Demonstration of the pre- and post-earthquake demand and capacity of the network.

in the entire network, which requires additional travel time compared to the pre-earthquake condition. The point E_0 in Fig. 4 is the equilibrium state in the pre-earthquake condition, where the pre-event demand curve meets the pre-event capacity curve. The point E_1 is, however, the equilibrium state in the post-earthquake condition, where the post-event demand and capacity curves intersect. Since the total travel time spent by drivers at the equilibrium condition can be considered as an indicator of total travel cost, the difference between the pre- and post-earthquake equilibrium conditions represents the extent of loss that the network experiences due to a specific earthquake event.

Based on the variable-demand model, the traffic is assigned to the transportation network so that the total travel time is minimized. To achieve this goal, the total travel time is obtained from the equilibrium model considering the flow and performance function of each link. Furthermore, the rates of travel between zone pairs are adjusted such that the travel demand on the entire network becomes consistent with the travel time. For this purpose, the trip rate for the purpose of p between origin zone, i, and destination zone, j, t_{ij}^p, is expressed as:

$$t_{ij}^p = O_i^P D_j^p K_{ij}^p \exp\left(\alpha^p + \beta^p c_{ij}\right) \text{ and } t_{ij}^p \geq 0 \;\forall\, i, j, p \tag{2}$$

where K_{ij}^p is the calibrated balancing coefficient for the trip purpose of p; α^p and β^p are the calibrated distance-decay coefficients for the trip purpose of p (Table 3); O_i^p is the trip generated from zone i; and D_j^p is the trip destined to zone j. When the network is subjected to an extreme event like an earthquake, the reduced trip parameters must be calculated using the reduction model as follows:

$$O_i^{a,p} = O_i^p\left(1 - \xi_i^p\right) \tag{3}$$

$$D_j^{a,p} = D_j^p\left(1 - \xi_j^p\right) \tag{4}$$

In Eq. (2), c_{ij} is the travel time between the OD pair of $i - j$, which is obtained from:

$$c_{ij} = \sum_l v_l r_l \delta_{ij}^{l,k} \tag{5}$$

where v_l is the traffic flow on the link l; r_l is the link performance function; k is the path connecting the OD zone; and $\delta_{ij}^{l,k}$ is an indicator variable, which is equal to one if the link l is on the path k between the OD zone and is equal to zero otherwise. The traffic flow on the link l, i.e., v_l, is calculated as:

$$v_l = \sum_p \sum_{i,j} \sum_k f_{ij}^{pk} \delta_{ij}^{l,k} \;\forall l \tag{6}$$

Table 3
Calibrated distance-decay coefficients for various trip purposes [37].

Trip Purpose	Time of Day	α	β	Trip purpose	Time of Day	α	β
Home-Work	Early Morning	3.152	−0.066	**Work-Other**	Early Morning	4.581	−0.150
	Midday	3.469	−0.102		Midday	3.971	−0.130
	Early Evening	3.170	−0.066		Early Evening	3.620	−0.084
	Night	3.539	−0.130		Night	4.447	−0.189
Home-School	Early Morning	4.288	−0.122	**Other-Other**	Early Morning	4.187	−0.119
	Midday	5.568	−0.270		Midday	4.546	−0.168
	Early Evening	4.544	−0.149		Early Evening	4.323	−0.125
	Night	5.856	−0.334		Night	4.847	−0.221
Home-Other	Early Morning	3.601	−0.083	**Truck Trips**	Early Morning	1.458	−0.024
	Midday	4.565	−0.173		Midday	1.531	−0.031
	Early Evening	4.279	−0.125		Early Evening	1.566	−0.026
	Night	4.966	−0.236		Night	1.350	−0.031

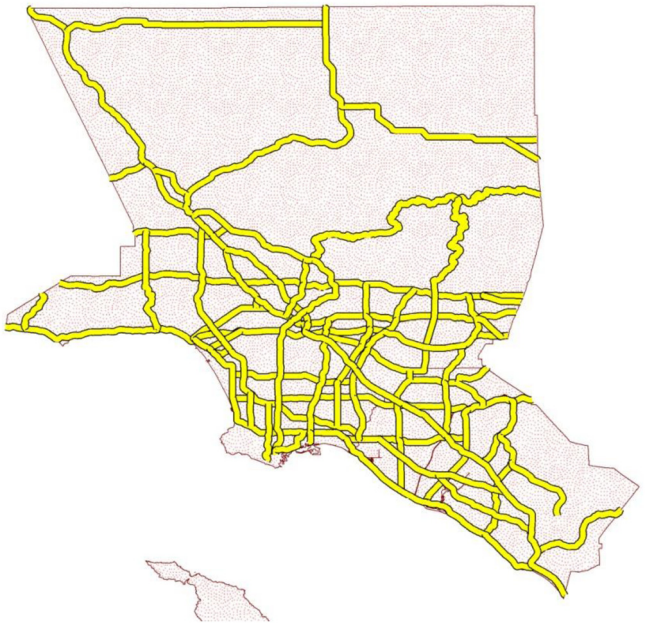

Fig. 5. Spatial distribution of the links in the transportation network of Los Angeles and Orange counties.

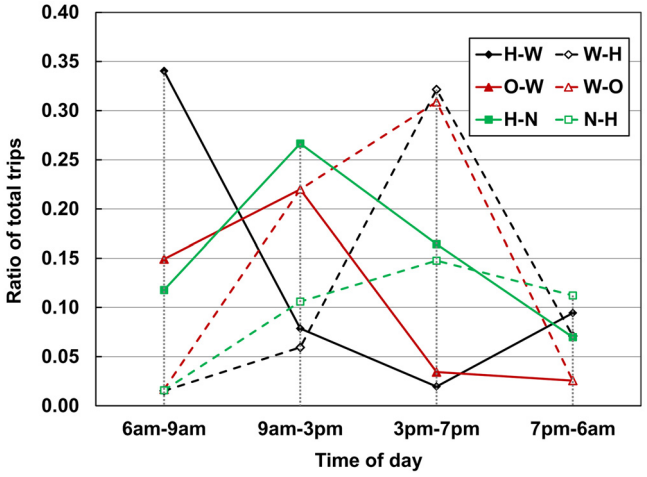

Fig. 6. Occurrence ratios of different trip purposes over a 24 h period.

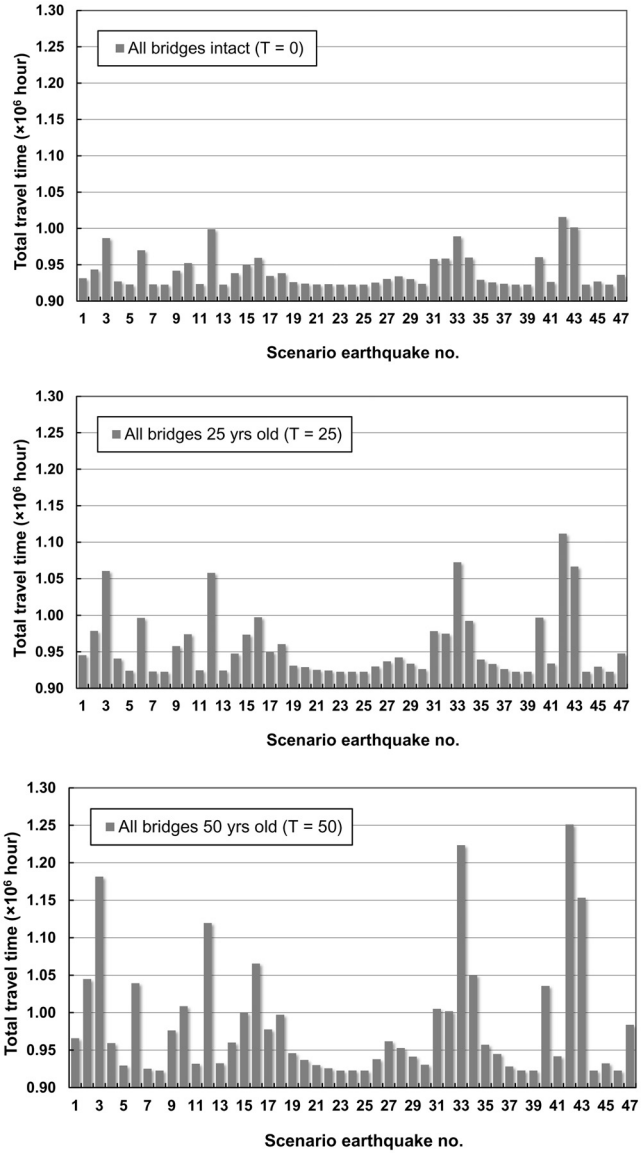

Fig. 7. Expected total travel time obtained for the transportation network subjected to scenario earthquakes.

where f_{ij}^{pk} is the flow of the trip purpose p on the path k between the $i-j$ pair. The flow information can be used to calculate:

$$t_{ij}^{p} = \sum_{k} f_{ij}^{pk} \quad \forall i, j, k, p \tag{7}$$

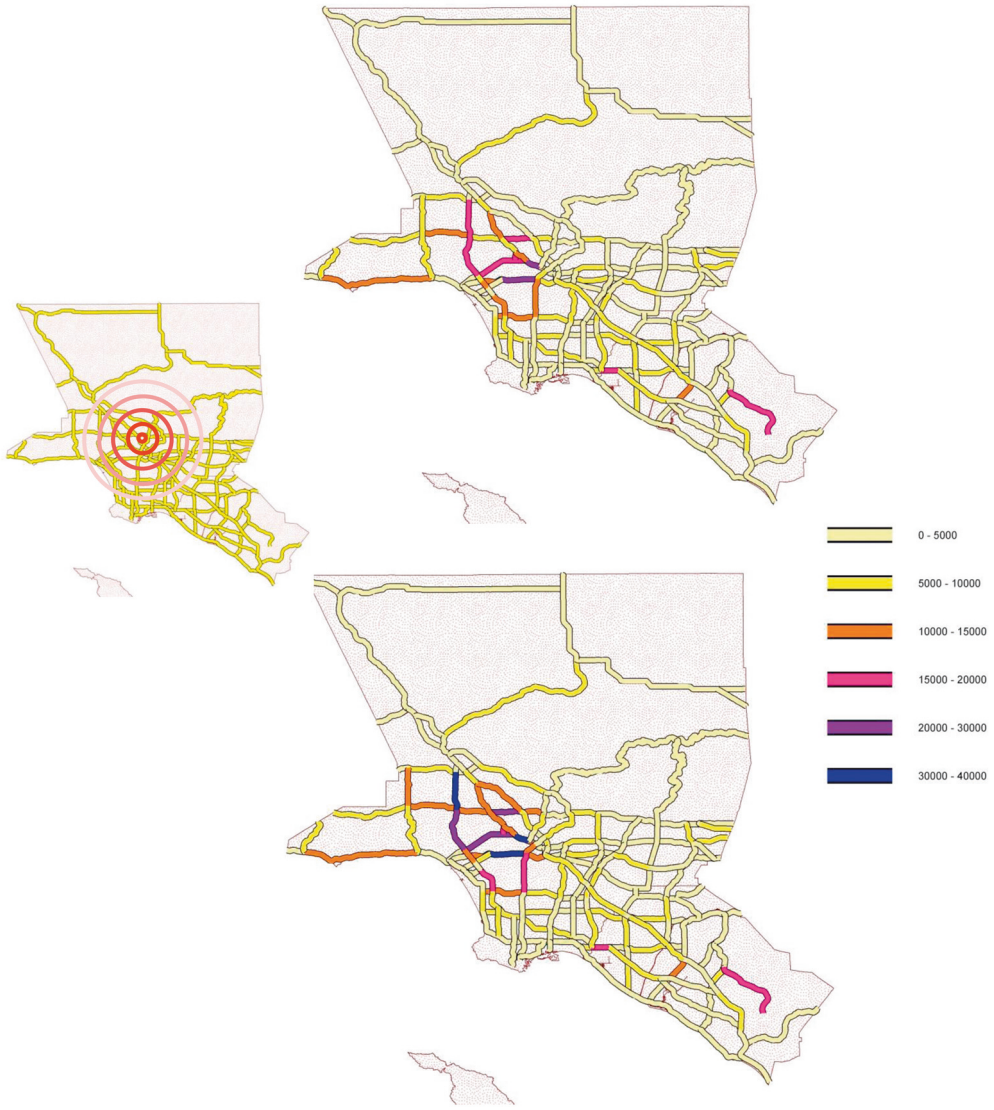

Fig. 8. Travel time in the individual links of the transportation network in the intact condition (top) and after 50 years (bottom) under No. 12 scenario earthquake.

Equations 2 through 7 form a recursive procedure, which requires a number of iterations to obtain the minimized total travel time.

6. Application to deteriorating transportation networks

The network of highway bridges in Los Angeles and Orange counties is investigated in the current study under the combined effects of environmental stressors and seismic events (Fig. 5). Since this network is modeled following the graph theory, each highway segment is represented by two oriented links (i.e., one for every direction of traffic). The points at which the links intersect are considered as nodes. To estimate the functionality measures of this network, the OD matrix is generated based on the data obtained for the local traffic analysis zones from the Southern California Association of Governments [43]. The traffic data for each analysis zone is condensed to the nodal OD data using the Thiessen polygons, following Zhou et al. [3]. Each Thiessen polygon defines an area of influence around its base point such that any location inside the polygon is closer to that point than to any of the other base points [44]. The condensed nodal OD data points are expressed in the form of square matrices with 148 rows and columns. Each matrix provides the information for one of the six general trip purposes (i.e., home-work, home-shop, home-other, work-other, other-other, and truck trips). It should be noted that the home-work matrix contains the data for both home-to-work and work-to-home trips. The other trip matrices are similar to the home-work matrix from this point of view.

The collected data for the matrices listed above includes the number of trips per day for the six trip purposes. Fig. 6 shows the occurrence ratios of different trip purposes over a 24 h period [37]. In this figure, each day has been divided into four time-windows, including: early morning (from 6 a.m. to 9 a.m.), midday (from 9 a.m. to 3 p.m.), early evening (from 3 p.m. to 7 p.m.), and night (from 7 p.m. to 6 a.m.). To provide more detailed information, the ratios calculated for the trips that include “home” have been separated to home-work (H-W and W-H) and home-nonwork (H-N and N-H), where nonwork covers both shop and other trips. In Fig. 6, the occurrence ratios for the trips related to work-other are shown by two separate lines, which represent both work-other (W-O) and other-work (O-W) trips. It is evident from this figure that the summation of each of the trip ratios is equal to 1.0 during each one-day period.

To demonstrate how the consequences of structural degradation can be integrated into the procedure developed for the resilience assessment of transportation networks subjected to extreme events, a series of aging scenarios are introduced for the network of Los Angeles and Orange counties. For this purpose, it is first assumed that all the network components are in the same age, starting from 0 (i.e., pristine condition) to

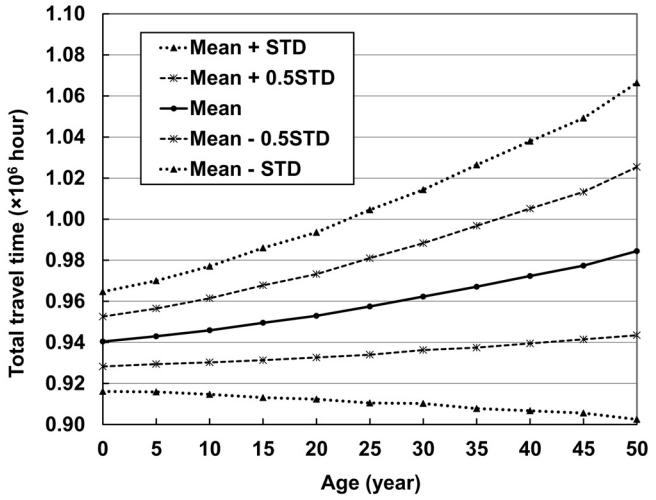

Fig. 9. Time-dependent changes of the mean and standard deviation (STD) of the total travel time.

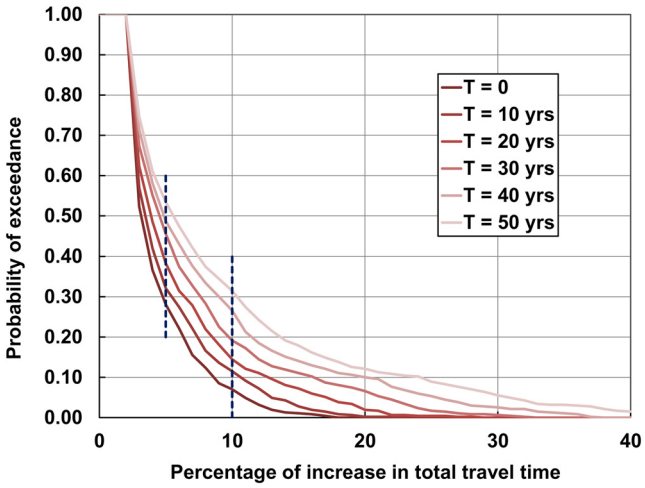

Fig. 10. Seismic risk curves generated for various stages of aging.

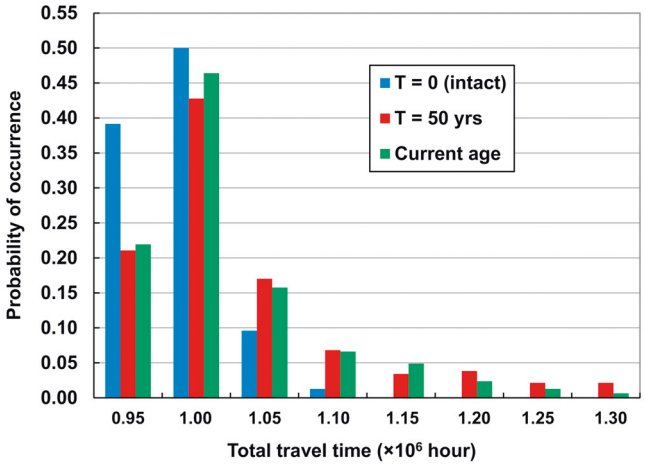

Fig. 11. Probability distribution of total travel time for the three aging scenarios considered in the current study.

75 years (i.e., expected design life). The seismic performance of the entire network is evaluated at regular time intervals considering the most current state of the individual components. This is achieved by updating the fragility measures of the existing bridges with the progress of deterioration. It is noted that the total travel time for the network in normal operation ($TT_{0,s}$) is approximately 900,000 h per day. This travel time, however, increases because of damage to the bridges and links when an earthquake occurs in the region. Fig. 7 shows the expected total travel time for the network of spatially distributed bridges, all of which at the same age. It is evident that if the contribution of aging mechanisms is neglected, the increased total travel time remains under 1,000,000 h per day for almost all the scenario earthquakes. However, this is not the case for the other two simulation scenarios, in which the age of bridges has changed to 25 and 50 years. A continuous exposure to aggressive environmental stressors has resulted in progressive structural degradation at the component level and increased seismic vulnerability at the network level. As a case in point, for the No. 12 scenario earthquake, which represents the Verdugo earthquake with the magnitude of 6.8, an increase of 5.80% and 11.96% in the total travel time is recorded for the network of 25- and 50-year old, respectively. Fig. 8 illustrates the travel time in the individual network links subjected to the same earthquake. This figure clearly shows how the extent and pattern of damage to the network change when the aging-related issues are taken into account.

Considering the total travel time obtained for various age and earthquake scenarios ($TT_{t,s}$), Fig. 9 provides a summary of the mean and standard deviation values calculated at 5-year time intervals. This figure indicates that, in addition to the mean, the standard deviation of the expected total travel time increases by time. This is mainly due to the uncertainties identified in the network's demand and capacity parameters. To further understand the probabilistic aspects of the predictions, a set of seismic risk curves are generated for the network under study at six time steps, following Eq. (1) (Fig. 10). Each curve represents the probability of exceeding a certain percentage of increase in the total travel time, given the network's deteriorating state. By introducing the critical total travel time, as a percentage of increase in the original total travel time (κ%), the network's functionality should be examined on a regular basis to determine the time of exceeding the critical level. Assuming that the maximum percentage of increase that can be tolerated is $\kappa = 10\%$, the probability of exceedance changes from 0.07 in the pristine network to 0.35 in the network made of 50-year old bridges. By employing a stricter threshold and limiting the maximum percentage of increase to $\kappa = 5\%$, the network is found to be more vulnerable with the probability of exceedance of 0.28 in the pristine network and 0.53 in the network made of 50-year old bridges (Fig. 10). Based on this information, the toleration limit can be adjusted further, depending on the needs/preferences of bridge owners and decision-making authorities.

In a real transportation network like the one that serves Los Angeles and Orange counties, not all the bridges are similarly aged. Alipour [28] conducted a study on the age of bridges in the region and found that the majority of them fall into the range of 30 to 60 years, with an average of 47 and standard deviation of close to 16 years. To capture the age variation factor, the performance of the network under consideration is examined assuming that the age of the existing bridges is a random variable with a distribution obtained from the age data extracted from the inventory of California bridges [45]. The total travel time for the network with actual age data is calculated under each of the scenario earthquakes. The probability distribution obtained for the total travel time is shown in Fig. 11 for the real age distribution, in addition to the pristine and identically aged ones. It is observed that this approach is capable of providing realistic predictions of the network's functionality, as it incorporates the latest condition of the individual bridges into the network-level analyses. The accuracy of such predictions can be further improved if the actual built year is assigned to each individual bridge.

7. Conclusions

A comprehensive framework for the life-time resilience assessment of deteriorating transportation networks was established through the

presented study. This framework is capable of taking into account the effects of (i) natural and manmade hazards, (ii) aging mechanisms and environmental stressors, and (iii) time-dependent structural degradation of individual network components. The network analyses conducted for this framework provide reliable predictions for a variety of functionality measures employed to ensure that the existing network can satisfy certain performance requirements, especially during extreme events. Among various extreme events, the main focus of this study was on the seismic damageability of transportation networks, as an earthquake event may impact a large geographic region in a short period of time. This situation may result in major network disruptions, depending on the extent of damage to the links and bridges. To quantify the seismic damageability of network components, a series of detailed FE analyses were conducted to determine the life-time safety and performance of the existing bridges under the combined effects of environmental stressors and earthquake loads. Utilizing the most current state of the network, an integrated traffic assignment model was used to account for fluctuations in the traffic demand in the aftermath of an earthquake event. This model considered six different trip purposes and identified the total travel time required for all the users of the network to get to their destinations. The total travel times obtained at different states of aging under different scenario earthquakes were employed as a performance indicator to measure the network's post-event functionality. A comparison between the results of this study with those without the consideration of deterioration effects indicated that the developed framework is capable of providing more realistic estimates of the performance of deteriorating networks after major earthquakes. With the potential of this framework to include other sources of environmental stressors and extreme events (depending on region-specific hazards), the outcome of this study can be of great value to bridge owners and decision-making authorities. In particular, this overarching framework can be employed to identify most appropriate future investments, plan for essential emergency routes, and decide on optimal resource allocation strategies for maintenance, repair, and strengthening purposes.

Declaration of Competing Interest

The authors declare that they have no known competing financial interests or personal relationships that could have appeared to influence the work reported in this paper.

Acknowledgements

The research study, results of which reported in this manuscript, was partially sponsored by the National Science Foundation (NSF) under Grants No. 2125426. The authors would like to acknowledge and thank the sponsor for this support. The first author would like to also thank Collegium Helveticum at ETH Zurich for their support. Opinions, findings, and conclusions expressed in this manuscript are of the authors and do not necessarily reflect those of the sponsors.

References

[1] Zhang Y, Ayyub B, Fung J. Projections of corrosion and deterioration of infrastructure in United States coasts under a changing climate. J Resilient Cities Struct 2022;1(1):98–109.
[2] Guikema S, Gardoni P. Reliability estimation for networks of reinforced concrete bridges. J Infrastruct Syst 2009;15(2):61–9.
[3] Zhou Y, Banerjee S, Shinozuka M. Socio-economic effect of seismic retrofit of bridges for highway transportation networks: a pilot study. J Struct Infrastruct Eng 2011;6(1–2):145–57.
[4] Chang L, Peng F, Ouyang Y, Elnashai AE, Spencer BF. Bridge seismic retrofit program to maximize post-earthquake transportation network capacity. J Infrastruct Syst 2012;18(2):75–88.
[5] Zhang N, Alipour A. Application of novel recovery techniques to enhance the resilience of transportation networks. Transp Res Record J Transp Res Board 2018;2672(1):138–47.
[6] Zhang N, Alipour A. Integrated framework for risk and resilience assessment of road network under inland flooding. Transp Res Record J Transp Res Board 2019;2673(12):182–90.
[7] Zhang N, Alipour A. Multi-scale robustness model for highway networks under flood events. Transp Res Part D Transport Environ 2020;83(102281):1–10.
[8] Li J, Gong J, Wang L. Seismic behavior of corrosion-damaged reinforced concrete columns strengthened using combined carbon fiber-reinforced polymer and steel jacket. J Const Build Mater 2009;23(7):2653–63.
[9] Simon J, Bracci JM, Gardoni P. Seismic response and fragility of deteriorated reinforced concrete bridges. J Struct Eng 2010;136(10):1273–81.
[10] Shafei B, Alipour A. Application of large-scale non-Gaussian stochastic fields for the study of corrosion-induced structural deterioration. J Eng Struct 2015;88:262–276.
[11] Shafei B, Alipour A. Estimation of corrosion initiation time in reinforced concrete bridge columns: how to incorporate spatial and temporal uncertainties. J Eng Mech 2015;141(10(04015037)):1–12.
[12] Khatami D, Shafei B, Smadi O. Management of bridges under aging mechanisms and extreme events: a risk-based approach. Transp Res Record J Transp Res Board 2016;2550(1):89–95.
[13] Kulkarni A, Shafei B. Impact of extreme events on transportation infrastructure in Iowa: a Bayesian network approach. Transp Res Record J Transp Res Board 2018;2672(48):45–57.
[14] Cui Z, Alipour A, Shafei B. Structural performance of deteriorating reinforced concrete columns under multiple earthquake events. J Eng Struct 2019;191:460–8.
[15] Zhang N, Alipour A. A two-level mixed-integer programming model for prioritization of bridge repair. J Comput Aided Civ Infrastruct Eng 2020;35(2):116–33.
[16] Alipour A, Shafei B, Shinozuka M. Performance evaluation of deteriorating highway bridges in high seismic areas. J Bridge Eng 2011;16(5):597–611.
[17] Lee YJ, Song J, Gardoni P, Lim HW. Post-hazard flow capacity of bridge transportation network considering structural deterioration of bridges. J Struct Infrastruct Eng 2010;7(7–8):509–21.
[18] Rokneddin K, Ghosh J, Dueñas-Osorio L, Padgett JE. Bridge retrofit prioritisation for ageing transportation networks subject to seismic hazards. J Struct Infrastruct Eng 2013;9(10):1050–66.
[19] Alipour A, Shafei B, Shinozuka M. Capacity loss evaluation of reinforced concrete bridges located in extreme chloride-laden environments. J Struct Infrastruct Eng 2013;9(1):8–27.
[20] Singh RR, Bruneau M, Stavridis A, Sett K. Resilience deficit index for quantification of resilience. J Resilient Cities Struct 2022;1(2):1–9.
[21] Castillo JG, Brunneau M, Elhami-Khorasani N. Seismic resilience of building inventory towards resilient cities. J Resilient Cities Struct 2022;1(1):1–12.
[22] Blagojevic N, Stojadinovic B. A demand-supply framework for evaluating the effect of resource and service constraints on community disaster resilience. J Resilient Cities Struct 2022;1(1):13–32.
[23] Shafei B, Alipour A, Shinozuka M. Prediction of corrosion initiation in reinforced concrete members subjected to environmental stressors: a finite-element framework. J Cem Concr Res 2012;42(2):365–76.
[24] HAZUS-MH Computer software. Washington, DC: Federal Emergency Management Agency (FEMA); 2010.
[25] Priestly MJN, Seible F, Calvi GM. Seismic design and retrofit of bridges. USA: John Wiley and Sons; 1996.
[26] Hwang, H., Liu, J.B., and Chiu, Y.H. (2001), *Seismic fragility analysis of highway bridges*, Report No. MAEC RR-4, Center for Earthquake Research and Information, University of Memphis, TN.
[27] Choi E, DesRoches R, Nielson B. Seismic fragility of typical bridges in moderate seismic zones. J Eng Struct 2004;26(2):187–99.
[28] Alipour A. Life-cycle performance assessment of highway bridges under multi-hazard conditions and environmental stressors, Irvine, CA: University of California; 2010. Ph.D. Dissertation, Department of Civil and Environmental Engineering.
[29] Alipour A, Shafei B, Shinozuka M. Structural seismic design optimization and earthquake engineering: formulations and applications. In: A multi-hazard framework for optimum life-cycle cost design of reinforced concrete bridges. IGI Global; 2012. p. 76–104. (Book Chapter) Published in.
[30] Shafei B. Stochastic finite-element analysis of reinforced concrete structures subjected to multiple environmental stressors, Irvine, CA: University of California; 2011. Ph.D. Dissertation, Department of Civil and Environmental Engineering.
[31] Shafei B, Alipour A, Shinozuka M. A stochastic computational framework to investigate the initial stage of corrosion in reinforced concrete superstructures. J Comput Aided Civ Infrastruct Eng 2013;28(7):482–94.
[32] Khatami D, Hajilar S, Shafei B. Investigation of oxygen diffusion and corrosion potential through a cellular automaton framework. J Corros Sci 2021;187(109496):1–10.
[33] Khatami D, Shafei B. Impact of climate conditions on deteriorating reinforced concrete bridges in the U.S. Midwest region. J Perform Constr Facil 2021;35(1):1–11 04020129.
[34] Alipour A, Shafei B, Shinozuka M. Performance evaluation of deteriorating highway bridges in high seismic areas. ASCE J Bridge Eng 2011;16(5):597–611.
[35] Shinozuka, M., Banerjee, S., and Kim, S.H. (2007), *Fragility considerations in highway bridge design*, Multidisciplinary center for earthquake engineering research, Buffalo, NY Report MCEER-07-0023.
[36] Chang SE, Shinozuka M, Moore J. Probabilistic earthquake scenarios: extending risk analysis methodologies to spatially distributed systems. Earthq Spectra 2000;16(3):557–72.
[37] Shiraki N, Shinozuka M, Moore J, Chang S, Kameda H, Tanaka S. System risk curves: probabilistic performance scenarios for highway networks subject to earthquake damage. J Infrastruct Syst 2007;13(1):43–54.
[38] Campbell KW, Bozorgnia Y. Campbell-Bozorgnia nga ground motion relations for the geometric mean horizontal component of peak and spectral ground motion parameters, Berkley, CA: Pacific Earthquake Engineering Research Center; 2007. Report No. 2007/02.

[39] Chang SE, Nojima N. Measuring lifeline system performance: highway transportation system in recent earthquakes. In: Proceedings of the 6th national conference on earthquake engineering, Oakland, CA; 1998. Paper No. 70, Earthquake Engineering Research Institute.
[40] Werner, S.D., Taylor, C.E., Cho, S., Lavoie, J.-.P., Huyck, C., Eitzel, C., Chung, H., and Eguchi, R.T. (2006), *REDARS 2: methodology and software for seismic risk analysis of highway systems*, Special Report No. MCEER- 06-SP08, Multidisciplinary Center for Earthquake Engineering Research, Buffalo, NY.
[41] Fan Y, Liu C, Lee R, Kiremidjian AS. Highway network retrofit under seismic hazard. J Infrastruct Syst 2010;16(3):181–7.
[42] Wardrop JG. Some theoretical aspects of road traffic research. In: Proceedings of the road engineering division meeting, 1; 1952. p. 325–62.
[43] SCAG (2007), Southern California association of governments, http://www.scag.ca.gov.
[44] ArcGIS (2008), Computer software, ESRI Inc., http://www.esri.com.
[45] NBI (2009), National bridge inventory, http://www.fhwa.dot.gov/bridge/nbi.